INTERNATIONAL JOURNAL FOR NUMERICAL METHODS IN FLUIDS, VOL. 4, 1083–1095 (1984)

ON THE CONSISTENCY OF FOUR DIFFERENT CONTROL SURFACES USED FOR FINITE AREA BLADE-TO-BLADE FLOW CALCULATIONS

T. ARTS

von Karman Institute for Fluid Dynamics, Chaussée de Waterloo, 72, B-1640 Rhode Saint Genèse, Belgium

SUMMARY

The aim of this contribution is to investigate the consistency and order of accuracy of different control surfaces used for finite area blade-to-blade flow calculations. The following cases will be treated: a hexagonal element, a trapezoidal element, a bitrapezoidal element and a quadrilateral element. Finally, the consistency conditions will be discussed and compared with respect to a cascade flow application.

KEY WORDS Turbomachines Finite Volume Consistency

INTRODUCTION

About ten years ago, the so-called finite area method was introduced by McDonald[1] in order to compute the two-dimensional, inviscid and adiabatic flow of a perfect gas in the blade-to-blade plane of a linear cascade. Since then, this method has found wide applications[2–9] and was even extended to a three-dimensional geometry both in cascades[4,10–15] and turbine or compressor stages.[16–18]

The finite area (or volume in three dimensions) approach is based on a numerical representation of conservation equations written in an integral form. The physical domain of the flow is divided into several control surfaces (or volumes) which exchange mass, momentum and energy. Hence, the main advantage of this method is that it remains very close to the physics of the problem. On the contrary, a finite difference approach would require a co-ordinate transformation, which is generally quite complicated for a cascade geometry, whereas the use of a finite element method involves a rather complex and heavy mathematical formulation.

The finite area approach is most generally coupled with a time marching numerical procedure which considers the solution of a steady problem as the asymptotic solution of the time dependent equations modelling this problem. The aim of this contribution is to study the consistency[19] and the order of accuracy of different spatial discretizations of the blade passage. As a result, and without losing any generality, the time dependent terms will not be considered in what follows.

DISCRETIZATION OF THE PARTIAL DIFFERENTIAL EQUATIONS

The equations expressing the conservation of mass, momentum and energy, as they hold for an inviscid flow, are the Euler equations. Written in a stationary form, in the case of a two-dimensional

0271–2091/84/11 1083–13$01.30

Received 12 February 1983
Revised 11 November 1983

geometry, we get:

$$\frac{\partial \mathbf{f}}{\partial x} + \frac{\partial \mathbf{g}}{\partial y} = 0 \tag{1}$$

$$\mathbf{f} = \begin{bmatrix} \rho u \\ \rho u^2 + p \\ \rho uv \\ u(\rho E + p) \end{bmatrix}, \qquad \mathbf{g} = \begin{bmatrix} \rho v \\ \rho uv \\ \rho v^2 + p \\ v(\rho E + p) \end{bmatrix}$$

If S is the area of a control surface, ∂S its perimeter and $\mathbf{n}$, with projections $\mathbf{n}_x$ and $\mathbf{n}_y$, the outward normal on ∂S, the integration of equation (1) over S, applying the Gauss theorem to the surface integrals, yields the following relation:

$$\int_{\partial S} \mathbf{f}(\mathbf{n}_x \cdot \mathbf{dl}) + \int_{\partial S} \mathbf{g}(\mathbf{n}_y \cdot \mathbf{dl}) = 0 \tag{2}$$

As will be shown for turbomachinery applications, the control surfaces are chosen to be almost regular polygons. Equation (2) can then be approximated by a sum of integrals, providing a suitable averaging of the flux terms $\mathbf{f}$ and $\mathbf{g}$ on each of the m sides of the polygons:

$$\sum_{l=1}^{m} \bar{\mathbf{f}}_l \int_{\partial S_l} \mathbf{n}_x \cdot \mathbf{dl} + \sum_{l=1}^{m} \bar{\mathbf{g}}_l \int_{\partial S_l} \mathbf{n}_y \cdot \mathbf{dl} = 0 \tag{3}$$

$$\sum_{l=1}^{m} \partial S_l = \partial S$$

Equation (3), where the ∂S_l represent the sides of the chosen control area, is going to be applied to study the consistency and the order of accuracy of different spatial discretizations. As will be seen in the next sections, the approximated flux terms of equation (3) result from quite simple relations, depending on the kind of control surface.

SPATIAL DISCRETIZATION OF THE BLADE PASSAGE

Two different kinds of grids are commonly used to discretize a blade passage. Although body-fitted meshes provide more accurate definition around leading and trailing edge, they require more involved programming work to be constructed. For this reason, we decided to use the very popular grid presented in Figure 1 because of its simplicity and flexibility. This grid is made up of several pseudo-streamlines and pitchwise lines. The pseudo-streamlines are uniformly spaced in the pitchwise (y) direction. The spacing between the pitchwise lines is regularly decreased from the inlet plane (AE) to the leading edge plane (BF) and regularly increased from the trailing edge plane (CG) to the outlet plane (DH) to avoid too many grid lines, and hence grid points, upstream and downstream of the cascade, in a region where less attention is paid to the flow, and, as a consequence, to limit the total computational time. Between leading and trailing edge, the spacing between the pitchwise lines is variable, depending on the required precision and the expected density gradients: a denser grid is used where more detailed information is desirable.

Obviously, several types of control surfaces can be constructed in this grid. Nevertheless, we decided to consider only the ones which, to our knowledge, are the most frequently encountered in aerodynamic blade performance analysis. They are presented in Figure 2: a hexagonal element used by McDonald,[1] Couston[2] and Lehthaus,[5] a trapezoidal element used by Denton[3,4] a

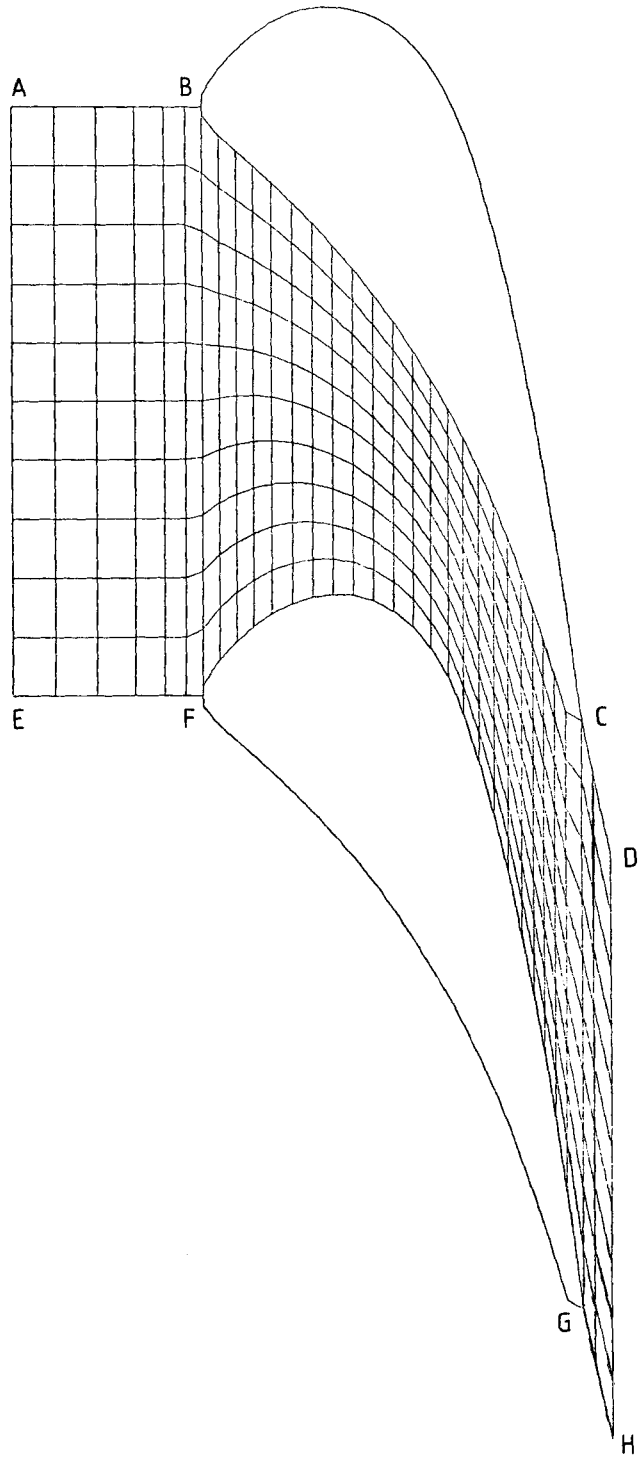

Figure 1. Numerical domain of the flow

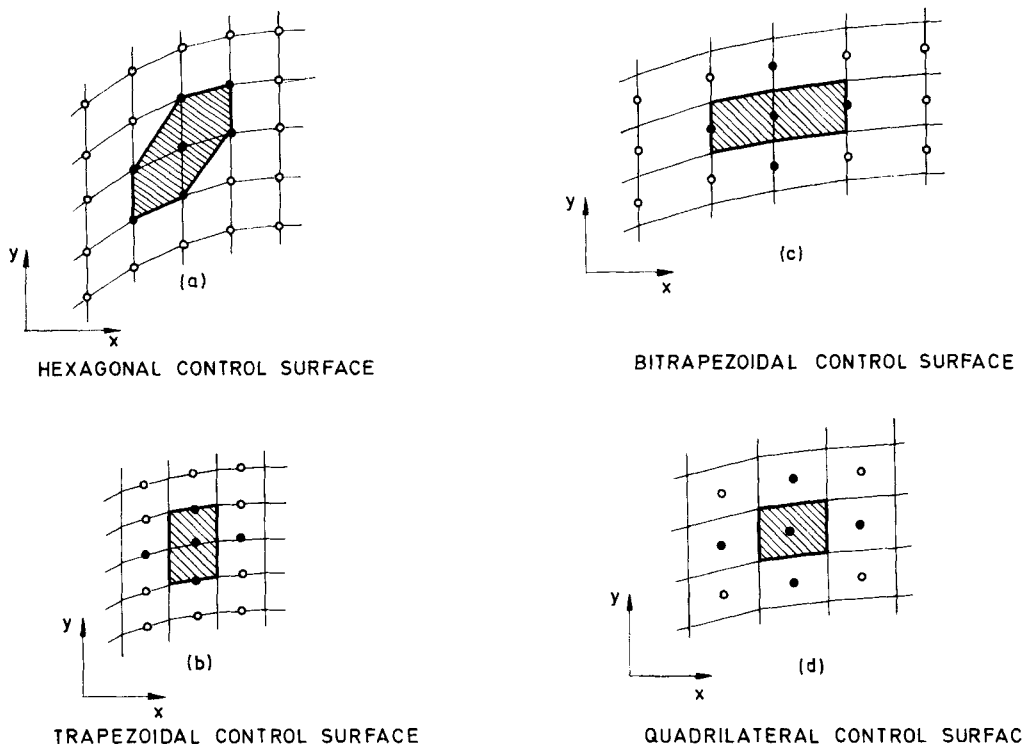

Figure 2. Description of the control surfaces

bitrapezoidal element used by Van Hove[6] and Arts[9,17] and a quadrilateral element used by Essers and Kafyeke.[7,8] We will now establish the conditions necessary to obtain with these elements a spatial discretization consistent with the initial partial differential system of equations (1).

Hexagonal control surface (McDonald)

The apices of the hexagons (nodes of the discretization) are located at the intersections of the grid lines. A linear variation of the flow quantities between two adjacent nodes is assumed in order to calculate the axial and tangential components of the mass-, momentum- and energy-transport terms through the different boundaries of the control surfaces. For two adjacent nodes, the surfaces overlap both in axial and tangential directions. The different geometrical parameters are described in Figure 3. The unknowns in the node (i, k) are computed from the corresponding values in the surrounding nodes A, B, C, D, E and F.

The application of equation (3) to this kind of element yields the following relation:

$$
\begin{aligned}
&-\tfrac{1}{2}(f_{i-1,k-1}+f_{i-1,k})\Delta y_1-\tfrac{1}{2}(f_{i-1,k}+f_{i,k+1})(\Delta y_2+\Delta y_4)\\
&+\tfrac{1}{2}(g_{i-1,k}+g_{i,k+1})\Delta x_1-\tfrac{1}{2}(f_{i,k+1}+f_{i+1,k+1})(\Delta y_3+\Delta y_5-\Delta y_2)\\
&+\tfrac{1}{2}(g_{i,k+1}+g_{i+1,k+1})\Delta x_2+\tfrac{1}{2}(f_{i+1,k+1}+f_{i+1,k})\Delta y_3\\
&+\tfrac{1}{2}(f_{i,k-1}+f_{i+1,k})(\Delta y_2+\Delta y_5)-\tfrac{1}{2}(g_{i,k-1}+g_{i+1,k})\Delta x_2\\
&+\tfrac{1}{2}(f_{i,k-1}+f_{i-1,k-1})(\Delta y_1+\Delta y_4-\Delta y_2)-\tfrac{1}{2}(g_{i,k-1}+g_{i-1,k-1})\Delta x_1=0
\end{aligned}
\tag{4}
$$

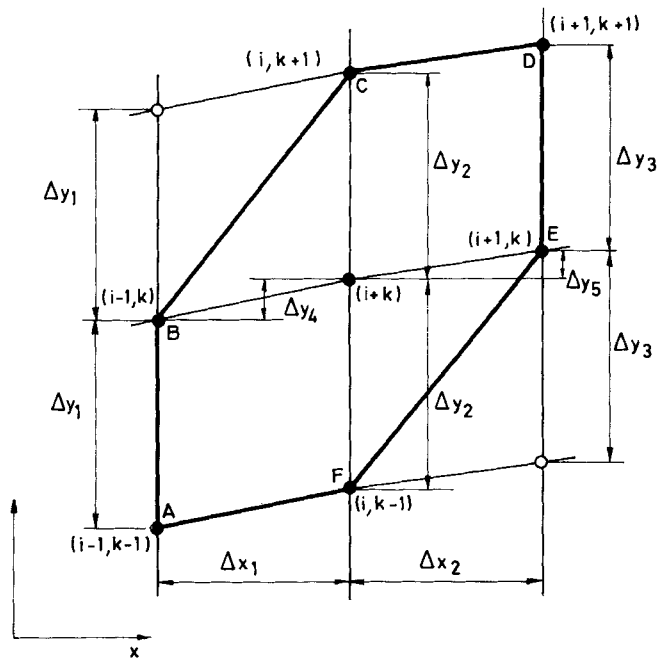

Figure 3. Hexagonal control surface (McDonald)

Expanding the different flux terms in Taylor series around the node (i, k), we get the following equation:

$$\left(\frac{\partial f}{\partial x}+\frac{\partial g}{\partial y}\right)(\Delta x_1\Delta y_1+\Delta x_2\Delta y_3+2\Delta y_2(\Delta x_1+\Delta x_2))$$
$$+\frac{\partial^2 f}{\partial x^2}[\tfrac{1}{2}(\Delta x_2^2\Delta y_3-\Delta x_1^2\Delta y_1)+\Delta y_2(\Delta x_2^2-\Delta x_1^2)]$$
$$+\frac{\partial^2 f}{\partial x\partial y}[2\Delta y_2(\Delta x_2\Delta y_5-\Delta x_1\Delta y_4)+\Delta y_2(\Delta x_2\Delta y_3-\Delta x_1\Delta y_1)]$$
$$+\frac{\partial^2 f}{\partial y^2}[\tfrac{1}{2}(\Delta y_1^2\Delta y_4-\Delta y_3^2\Delta y_5)+\tfrac{1}{2}(\Delta y_4^2\Delta y_1-\Delta y_5^2\Delta y_3)+\tfrac{1}{2}\Delta y_2^2(\Delta y_1-\Delta y_3)$$
$$+\Delta y_2(\Delta y_5^2-\Delta y_4^2)+\tfrac{1}{2}\Delta y_2(\Delta y_3^2-\Delta y_1^2)+\Delta y_2(\Delta y_3\Delta y_5-\Delta y_1\Delta y_4)]$$
$$+\frac{\partial^2 g}{\partial y^2}[\tfrac{1}{2}(\Delta y_3^2\Delta x_2-\Delta y_1^2\Delta x_1)+(\Delta x_2\Delta y_3\Delta y_5-\Delta y_1\Delta x_1\Delta y_4)]$$
$$+\frac{\partial^2 g}{\partial x\partial y}(\Delta x_2^2\Delta y_3-\Delta x_1^2\Delta y_1)+O(\Delta^4)=0 \tag{5}$$

When the Δx_j and Δy_j tend uniformly towards 0, equation (4) can be condensed as follows:

$$\left(\frac{\partial f}{\partial x}+\frac{\partial g}{\partial y}\right)+\frac{O(\Delta^3)\cdot\text{second derivatives}}{O(\Delta^2)}+O(\Delta^2)=0 \tag{6}$$

which is equivalent to equation (1) plus a first-order term. Thus, the discretization obtained with a hexagonal element is consistent with the partial differential system to be solved and is at least first-order accurate. To get a second-order accuracy at the point (i, k), the following conditions must be fulfilled:

$$\left.\begin{aligned} \Delta y_1 - \Delta y_3 &= O(\Delta^2) \\ \Delta y_4 - \Delta y_5 &= O(\Delta^2) \\ \Delta x_1 - \Delta x_2 &= O(\Delta^2) \end{aligned}\right\} \tag{7}$$

These conditions may allow some kind of periodically distorted mesh in the pitchwise direction; as a matter of fact, no specific relation is imposed between Δy_1 and Δy_2. But as our interest is in the area of blade-to-blade flow calculation in a realistic turbomachinery geometry, equation (7) can be generalized by requiring a regular mesh with at most small slope variations of the pseudo streamlines and nearly constant spacing between the pitchwise lines.

Trapezoidal control surface (Denton)

The nodes at which the unknowns are computed are located on the pseudo-streamlines, halfway between two pitchwise lines. For two consecutive grid points the control surfaces overlap only in tangential direction. The different geometrical parameters are described in Figure 4. The unknowns at the node (i, k) are computed from the corresponding values at the surrounding nodes $(i, k+1)$, $(i+1, k)$ $(i, k-1)$ and $(i-1, k)$.

The fluxes are considered to be uniform along the boundaries AB, BC, CD and DA. Along AB and CD, the transport terms are computed from the flow values in the nodes located on both sides

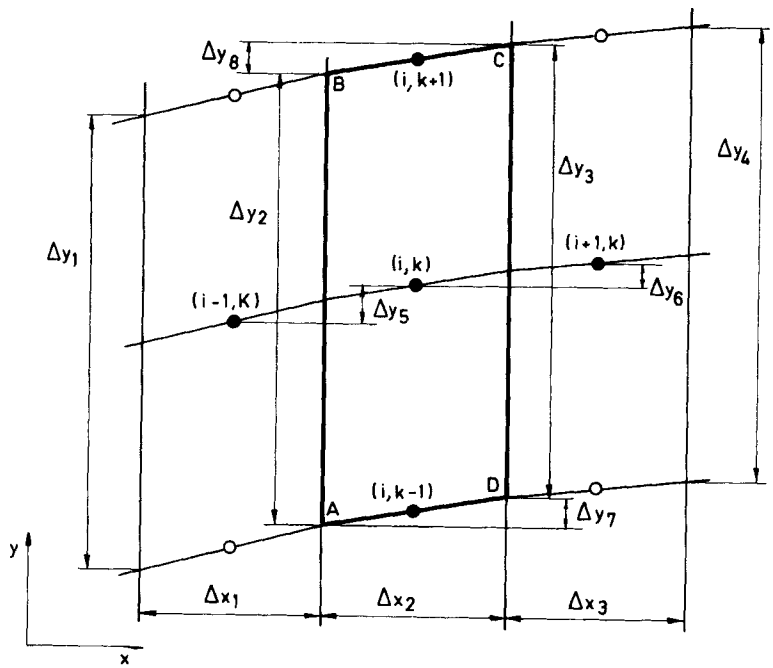

Figure 4. Trapezoidal control surface (Denton)

of those boundaries whereas along BC and DA, the fluxes are calculated using the values at the nodes located on those boundaries. Using a weighted average, the application of equation (3) to this kind of element yields the following relation:

$$-\frac{f_{i-1,k}\Delta x_2 + f_{i,k}\Delta x_1}{\Delta x_1 + \Delta x_2}\Delta y_2 + \frac{f_{i,k}\Delta x_3 + f_{i+1,k}\Delta x_2}{\Delta x_2 + \Delta x_3}\Delta y_3 + (g_{i,k+1} - g_{i,k-1})\Delta x_2 + f_{i,k-1}\Delta y_7 - f_{i,k+1}(\Delta y_3 - \Delta y_2 + \Delta y_7) = 0 \tag{8}$$

Expanding the different flux terms in Taylor series around the node (i, k), we get the following equation:

$$\begin{aligned}
&\left(\frac{\partial f}{\partial x} + \frac{\partial g}{\partial y}\right)\left(\tfrac{1}{2}\Delta x_2(\Delta y_2 + \Delta y_3)\right) + \frac{\partial f}{\partial y}\left[\Delta y_2\left(\frac{\Delta x_2 \Delta y_5}{\Delta x_1 + \Delta x_2} - \frac{\Delta y_7 + \Delta y_8}{4}\right)\right. \\
&\quad \left. + \Delta y_3\left(\frac{\Delta x_2 \Delta y_6}{\Delta x_2 + \Delta x_3} - \frac{\Delta y_7 + \Delta y_8}{4}\right)\right] \\
&\quad + \frac{\partial^2 f}{\partial x^2}\left[-\tfrac{1}{8}\Delta x_2(\Delta y_2(\Delta x_1 + \Delta x_2) - \Delta y_3(\Delta x_2 + \Delta x_3))\right] \\
&\quad + \frac{\partial^2 f}{\partial x \partial y}\left(-\tfrac{1}{2}\Delta x_2(\Delta y_2 \Delta y_5 - \Delta y_3 \Delta y_6)\right) \\
&\quad + \frac{\partial^2 f}{\partial y^2}\left[-\tfrac{1}{2}\Delta x_2\left(\frac{\Delta y_2 \Delta y_5^2}{\Delta x_1 + \Delta x_2} - \frac{\Delta y_3 \Delta y_6^2}{\Delta x_2 + \Delta x_3}\right)\right. \\
&\quad \left. - \tfrac{1}{32}(\Delta y_2 + \Delta y_3)^2(\Delta y_2 - \Delta y_3)\right] + O(\Delta^4) = 0
\end{aligned} \tag{9}$$

When the Δx_j and Δy_j tend uniformly towards 0, and if the following conditions are satisfied:

$$\left.\begin{aligned}
\frac{\Delta x_2 \Delta y_5}{\Delta x_1 + \Delta x_2} - \frac{\Delta y_7 + \Delta y_8}{4} &= O(\Delta^2) \\
\frac{\Delta x_2 \Delta y_6}{\Delta x_2 + \Delta x_3} - \frac{\Delta y_7 + \Delta y_8}{4} &= O(\Delta^2)
\end{aligned}\right\} \tag{10}$$

then equation (9) can be condensed as equation (6) which is equivalent to equation (1) plus a first-order term. In view of equation (10), the discretization obtained with this trapezoidal element is only conditionally consistent with equation (1) and in general first-order accurate. In the case of a blade-to-blade flow calculation, it would not be acceptable that the discretization would impose a definite relation between the Δx_j and Δy_j. For this reason, equation (10) may be expressed in a more severe form:

$$\left.\begin{aligned}
\Delta x_1 - \Delta x_2 &= O(\Delta^2) \\
\Delta x_2 - \Delta x_3 &= O(\Delta^2) \\
2\Delta y_5 - (\Delta y_7 + \Delta y_8) &= O(\Delta^2) \\
2\Delta y_6 - (\Delta y_7 + \Delta y_8) &= O(\Delta^2)
\end{aligned}\right\} \tag{11}$$

To get a second-order accuracy at point (i, k), the following conditions must be satisfied:

$$\left.\begin{aligned} \frac{\Delta x_2 \Delta y_5}{\Delta x_1 + \Delta x_2} - \frac{\Delta y_7 + \Delta y_8}{4} &= O(\Delta^3) \\ \frac{\Delta x_2 \Delta y_6}{\Delta x_2 + \Delta x_3} - \frac{\Delta y_7 + \Delta y_8}{4} &= O(\Delta^3) \\ \Delta y_2 - \Delta y_3 &= O(\Delta^2) \\ \Delta y_5 - \Delta y_6 &= O(\Delta^2) \end{aligned}\right\} \tag{12}$$

For the reasons mentioned above, in the particular case of a blade channel geometry, equation (12) can be replaced by

$$\left.\begin{aligned} \Delta y_2 - \Delta y_3 &= O(\Delta^2) \\ \Delta y_5 - \Delta y_6 &= O(\Delta^3) \\ \Delta x_1 - \Delta x_2 &= O(\Delta^3) \\ \Delta x_2 - \Delta x_3 &= O(\Delta^3) \\ 2\Delta y_5 - (\Delta y_7 + \Delta y_8) &= O(\Delta^3) \\ 2\Delta y_6 - (\Delta y_7 + \Delta y_8) &= O(\Delta^3) \end{aligned}\right\} \tag{13}$$

These conditions express the fact that the grid has to be almost regular.

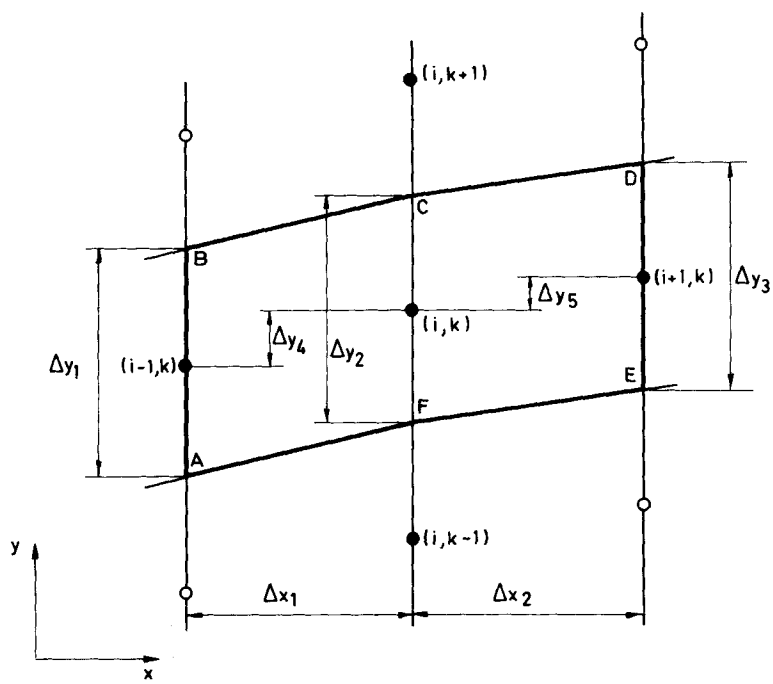

Figure 5. Bitrapezoidal control surface (Van Hove–Arts)

Bitrapezoidal control surface (Van Hove–Arts)

The nodes at which the unknowns are computed are located on the pitchwise lines, half-way between the pseudo-streamlines. For two consecutive nodes, the control surfaces overlap in the axial direction and not in the tangential direction. The different geometrical parameters are described in Figure 5. The unknowns at the node (i, k) are computed from the corresponding values at the surrounding nodes $(i, k+1)$, $(i+1, k)$, $(i, k-1)$ and $(i-1, k)$.

The fluxes are considered to be uniform along the boundaries AB, BCD, DE and EFA. Along BCD and EFA, the transport terms are computed from the flow values at the nodes located on both sides of these boundaries, whereas along AB and DE the fluxes are calculated using the values in the nodes located on these boundaries. The application of equation (3) to this kind of element yields the following relation:

$$\begin{aligned}
&-f_{i-1,k}\Delta y_1 - \tfrac{1}{2}(f_{i,k}+f_{i,k+1})\left(\frac{\Delta y_3}{2}+\Delta y_5-\frac{\Delta y_1}{2}+\Delta y_4\right)\\
&+\tfrac{1}{2}(g_{i,k}+g_{i,k+1})(\Delta x_1+\Delta x_2)+f_{i+1,k}\Delta y_3\\
&+\tfrac{1}{2}(f_{i,k}+f_{i,k-1})\left(\frac{\Delta y_1}{2}+\Delta y_4-\frac{\Delta y_3}{2}+\Delta y_5\right)\\
&-\tfrac{1}{2}(g_{i,k}+g_{i,k-1})(\Delta x_1+\Delta x_2)=0
\end{aligned} \tag{14}$$

Expanding the different flux terms in Taylor series around the node (i, k), we get the following equation:

$$\begin{aligned}
&\frac{\partial f}{\partial x}(\Delta y_3\Delta x_2+\Delta x_1\Delta y_1)+\frac{\partial g}{\partial y}(\Delta y_2(\Delta x_1+\Delta x_2))\\
&\quad+\frac{\partial f}{\partial y}(\Delta y_5(\Delta y_3-\Delta y_2)-\Delta y_4(\Delta y_2-\Delta y_1))+\frac{\partial^2 f}{\partial x^2}(\tfrac{1}{2}(\Delta y_3\Delta x_2^2-\Delta y_1\Delta x_1^2))\\
&\quad+\frac{\partial^2 f}{\partial y^2}(\tfrac{1}{2}(\Delta y_3\Delta y_5^2-\Delta y_1\Delta y_4^2))+\frac{\partial^2 f}{\partial x\partial y}(\Delta x_2\Delta y_3\Delta y_5-\Delta x_1\Delta y_1\Delta y_4)\\
&\quad+O(\Delta^4)=0
\end{aligned} \tag{15}$$

When the Δx_j and Δy_j tend uniformly towards 0, and if the following conditions are satisfied:

$$\left.\begin{aligned}
\Delta x_2(\Delta y_3-\Delta y_2)-\Delta x_1(\Delta y_2-\Delta y_1)&=O(\Delta^3)\\
\Delta y_5(\Delta y_3-\Delta y_2)-\Delta y_4(\Delta y_2-\Delta y_1)&=O(\Delta^3)
\end{aligned}\right\} \tag{16}$$

then equation (15) can be condensed as equation (6) which is equivalent to equation (1) plus a first-order term. In view of equation (16), the discretization obtained with a bitrapezoidal element is only conditionally consistent with (1) and first-order accurate in general. As the spatial increments must be independent in the x and y directions for a turbomachinery application, equation (16) may be written in the following form:

$$\begin{aligned}
\Delta y_3-\Delta y_2&=O(\Delta^2)\\
\Delta y_2-\Delta y_1&=O(\Delta^2)
\end{aligned} \tag{17}$$

To get a second-order accuracy at point (i, k), the following conditions must be fulfilled:

$$\left.\begin{aligned} \Delta x_2(\Delta y_3 - \Delta y_2) - \Delta x_1(\Delta y_2 - \Delta y_1) &= O(\Delta^4) \\ \Delta y_5(\Delta y_3 - \Delta y_2) - \Delta y_4(\Delta y_2 - \Delta y_1) &= O(\Delta^4) \\ \Delta y_3 - \Delta y_1 &= O(\Delta^2) \\ \Delta x_2 - \Delta x_1 &= O(\Delta 2) \\ \Delta y_5 - \Delta y_4 &= O(\Delta^2) \end{aligned}\right\} \tag{18}$$

In the particular case of a blade-to-blade flow calculation, equations (18) may be expressed as:

$$\left.\begin{aligned} \Delta y_3 - \Delta y_2 &= O(\Delta^3) \\ \Delta y_2 - \Delta y_1 &= O(\Delta^3) \\ \Delta y_4 - \Delta y_5 &= O(\Delta^2) \\ \Delta x_1 - \Delta x_2 &= O(\Delta^2) \end{aligned}\right\} \tag{19}$$

which impose some kind of almost regular grid.

Quadrilateral control surface (Essers–Kafyeke)

The nodes at which the unknowns are computed are located in the centre of each control surface. These surfaces overlap neither in the axial nor in the tangential direction. The different geometrical parameters are described in Figure 6. The unknowns at the node (i, k) are computed from the values at the surrounding nodes $(i, k+1)$, $(i+1, k)$, $(i, k-1)$ and $(i-1, k)$.

The fluxes are considered to be uniform along the boundaries AB, BC, CD and DA. Through these boundaries, the transport terms are computed as arithmetical mean values between the fluxes at the nodes located on each side of the considered boundaries. The application of equation (3) to

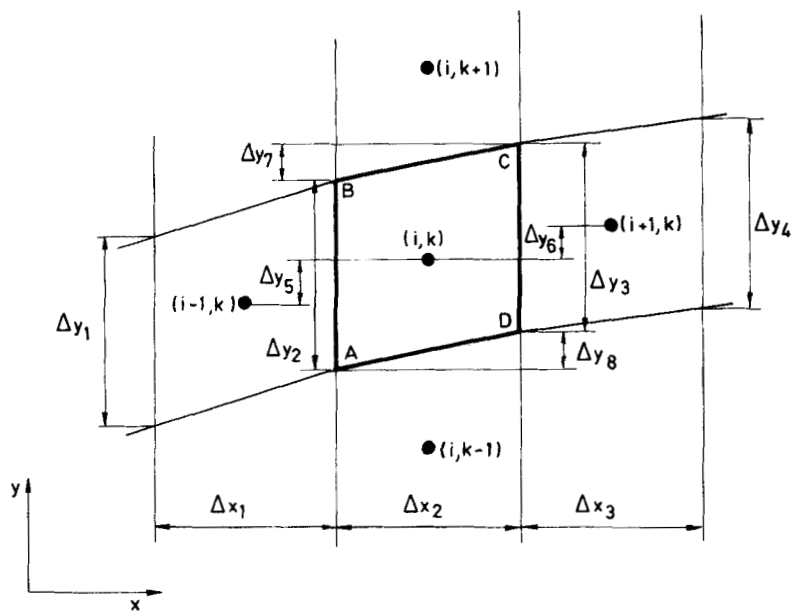

Figure 6. Quadrilateral control surface (Essers–Kafyeke)

this kind of element yields the following relation:

$$-\tfrac{1}{2}(f_{i-1,k}+f_{i,k})\Delta y_2-\tfrac{1}{2}(f_{i,k+1}+f_{i,k})\Delta y_7+\tfrac{1}{2}(g_{i,k}+g_{i,k+1})\Delta x_2$$
$$+\tfrac{1}{2}(f_{i,k}+f_{i+1,k})\Delta y_3+\tfrac{1}{2}(f_{i,k}+f_{i,k-1})(\Delta y_2-\Delta y_3+\Delta y_7)$$
$$-\tfrac{1}{2}(g_{i,k}+g_{i,k-1})\Delta x_2=0 \tag{20}$$

Expanding the different flux terms in Taylor series around the node (i,k), we get the following equation:

$$\frac{\partial f}{\partial x}[\tfrac{1}{2}(\Delta y_2(\Delta x_1+\Delta x_2)+\Delta y_3(\Delta x_2+\Delta x_3))]+\frac{\partial g}{\partial y}(\Delta x_2(\Delta y_2+\Delta y_3))$$
$$+\frac{\partial f}{\partial y}[\tfrac{1}{2}\Delta y_2(2\Delta y_5-\Delta y_7-\Delta y_8)+\tfrac{1}{2}\Delta y_3(2\Delta y_6-\Delta y_7-\Delta y_8))$$
$$+\frac{\partial^2 f}{\partial x^2}[\tfrac{1}{8}(\Delta y_3(\Delta x_2+\Delta x_3)^2-\Delta y_2(\Delta x_1+\Delta x_2)^2)]$$
$$+\frac{\partial^2 f}{\partial x\partial y}[\tfrac{1}{2}(\Delta y_3\Delta y_6(\Delta x_2+\Delta x_3)-\Delta y_2\Delta y_5(\Delta x_1+\Delta x_2))]$$
$$+\frac{\partial^2 f}{\partial y^2}(\tfrac{1}{2}(\Delta y_3\Delta y_6^2-\Delta y_2\Delta y_5^2)+\tfrac{1}{8}(\Delta y_2+\Delta y_3)^2(\Delta y_2-\Delta y_3))+O(\Delta^4)=0 \tag{21}$$

When the Δx_j and Δy_j tend uniformly towards 0, and if the following conditions are satisfied:

$$\Delta y_2(\Delta x_1-\Delta x_2)-\Delta y_3(\Delta x_2-\Delta x_3)=O(\Delta^3)$$
$$\Delta y_2(2\Delta y_5-\Delta y_7-\Delta y_8)+y_3(2\Delta y_6-\Delta y_7-\Delta y_8)=O(\Delta^3) \tag{22}$$

then equation (21) can be condensed as equation (6), which is equivalent to equation (1) plus a first-order term. In view of equation (22), the discretization obtained with this quadrilateral element is only conditionally consistent with equation (1) and first-order accurate in general. As no relation may exist between the Δx_j and Δy_j in the case of a blade to blade flow calculation, equation (22) may be expressed in the same way as equation (11).

To get a second-order accuracy at point (i,k), the following conditions must be fulfilled.

$$\left.\begin{aligned}\Delta y_2(\Delta x_1-\Delta x_2)-\Delta y_3(\Delta x_2-\Delta x_3)&=O(\Delta^4)\\ \Delta y_2(2\Delta y_5-\Delta y_7-\Delta y_8)+\Delta y_3(2\Delta y_6-\Delta y_7-\Delta y_8)&=O(\Delta^4)\\ \Delta y_3-\Delta y_2&=O(\Delta^2)\\ \Delta y_6-\Delta y_5&=O(\Delta^2)\\ \Delta x_3-\Delta x_1&=O(\Delta^2)\end{aligned}\right\} \tag{23}$$

For the particular case of a blade channel geometry, equation (23) can be transformed in the same way as equation (13); again an almost regular grid is required.

RESULTS

The different analyses we have done in the previous sections allow the evaluation of the consistency and the order of accuracy of different spatial discretizations proposed by various authors. The discretization obtained with the hexagonal control surface is unconditionally consistent with equation (1) and generally first-order accurate; six surrounding nodes are involved in the

computation of the unknowns at one grid point. In order to decrease the number of nodes involved in one control surface and thereby to reduce the total computational time, elements using four points were investigated. The consistency of the discretizations obtained with these elements is only conditional.

Concerning the trapezoidal and quadrilateral control surfaces, we have shown that a consistency error, which could become important, arises when sensible variations occur either in the slope of the pseudo-streamlines or in the spacing between the pitchwise lines, equation (11). The former could be encountered for a high cambered blade or in the leading and trailing edge regions whereas the latter are almost unavoidable in the case of a blade with a large outlet angle (with respect to the axial direction) where such variations are introduced in order to limit the streamwise over pitchwise distortions of the control surfaces in the rear part of the blade passage. The condition (11) could also theoretically explain why Denton[3,4] uses cusps to discretize the leading and trailing edge to get a smoother variation in the slope of the pseudo-streamlines in these regions. On the other hand, providing a first-order accurate discretization, no consistency error would be introduced by the computation of the flow in a passage presenting axial variations in the pitchwise distance between suction side and pressure side.

Concerning the bitrapezoidal control surfaces, in the general case of a first-order accurate discretization, no consistency error will occur because of variations in the slope of the pseudo streamlines or in the spacing between the pitchwise lines. But contrary to the two other 'four nodes' elements, the existence of a strong axial variation in the pitchwise distance between suction side and pressure side could be responsible for such an error (17), especially around the leading and trailing edge. This is the reason why a blunt discretization is applied in these regions.[9] According to this, it seems that the least severe condition to be fulfilled to insure consistency is related to the discretization obtained with the bitrapezoidal control surface (17).

CONCLUSION

The consistency and the order of accuracy of different spatial discretizations frequently applied to finite area cascade flow calculations were investigated. The discretization obtained with a hexagonal control surface is unconditionally consistent with the partial differential system to be solved and first-order accurate in general. Because of computational time requirements, three 'four nodes' control surfaces were also considered: trapezoidal, bitrapezoidal and quadrilateral. The consistency of the discretizations obtained with these elements is only conditional and, if consistent, generally first-order accurate. As far as our interest is in the area of blade to blade flow calculations, it appears that the use of the bitrapezoidal element imposes less severe restrictions on the geometry of the control surface than in the two other cases.

LIST OF SYMBOLS

c_v	specific heat at constant volume
$\mathbf{dl}$	length element on the perimeter of the control surface
E	total energy $[E = c_v T + (u^2 + v^2)/2]$
f	flux term of the conservative Euler system of equations
g	flux term of the conservative Euler system of equations
$\mathbf{n}$	outward normal on a control surface
$O(\ )$	of the order of
p	pressure
S	area of a control surface

T	temperature
u	axial velocity
v	tangential (or pitchwise) velocity
x	axial co-ordinate
y	tangential (or pitchwise) co-ordinate
$\Delta x, \Delta y$	spatial increments
ρ	density
∂S	perimeter of the control surface S

Subscripts

i, k	spatial indices (axial and tangential direction)

Superscripts

$\overline{}$	mean value

REFERENCES

1. P. W. McDonald, 'The computation of transonic flow through two dimensional gas turbine cascades', *ASME Paper* 71 GT 89, March 1971.
2. M. Couston, 'Méthode de calcul de l'écoulement inter-aubes pseudo tridimensionnel en régime transsonique', *Ph.D. Thesis* Université Libre de Bruxelles, September 1976.
3. J. D. Denton, 'Extension of the finite area time marching method to three dimensions', *Transonic Flow in Turbomachinery*, VKI LS 84, February 1976.
4. J. D. Denton and U. K. Singh, 'Time marching methods for turbomachinery calculations', *Application of Numerical Methods to Flow Calculations in Turbomachines*, VKI LS 1979–7, April 1979.
5. F. Lehthaus, 'Anwendung eines Zeitt-Schritt-Verfahrens zur Berechnung der transsonischen Durchströmung ebener turbinen-gitter und experimentelle Überprüfung', *DFVLR* 251 77 A 01, February 1977.
6. W. Van Hove, 'Time marching methods for turbomachinery flow calculations: methods of improving convergence', *Application of Numerical Methods to Flow Calculations in Turbomachines*, VKI LS 1979–7, April 1979.
7. J. A. Essers and F. Kafyeke, 'A new fast artificial evolution numerical method for transonic flows in turbine cascades', *VKI TN* 136, December 1980.
8. J. A. Essers and F. Kafyeke, 'Application of a fast pseudo unsteady method to steady transonic flows in turbine cascades', *ASME Paper* 81-GT-124, March 1981.
9. T. Arts, 'Cascade flow calculations using a finite volume method', *Numerical Methods for Flows in Turbomachinery Bladings*, VKI LS 1982–5, April 1982.
10. W. T. Thompkins and D. A. Oliver, 'Three dimensional flow calculation for a transonic compressor rotor', *Through Flow Calculations in Axial Turbomachinery*, AGARD CP 195, Paper 6, May 1976.
11. C. Bosman and J. Highton, 'A calculation procedure for three dimensional time dependent, inviscid, compressible flow through turbomachine blades of any geometry', *J. Mech. Eng. Sc.* **21,** (1), 39–49 (1979).
12. J. Brochet *et al.*, 'Calcul de l'écoulement tridimensionnel dans une roue mobile de soufflante. Mise en oeuvre sur un calculateur parallèle', *ONERA TP* 1981–20.
13. K. P. Sarathy, 'Computation of three dimensional flow fields through rotating blade rows and comparison with experiment. *ASME Trans., A—J. Eng. Power*, **104,** (2), 394–402 (1982).
14. W. T. Thompkins, 'A FORTRAN program for calculating three dimensional, inviscid, rotational flows with shock waves in axial compressor blade rows', *NASA CR* 3560, June 1982.
15. W. Van Hove, 'The calculation of three dimensional, inviscid, rotational flow in axial turbine blade rows', *ASME Paper* 83-GT-119, 1983. Also, VKI Preprint 1982–35.
16. C. Bosman, 'Inviscid three dimensional flow calculation in blade rows and stages (finite volume method)'. *Numerical Methods for Flows in Turbomachinery Bladings*, VKI LS 1982–5. April 1982.
17. T. Arts, 'Etude de l'écoulement tridimensionnel dans un étage de turbine transsonique', *Ph.D. Thesis*, U. Catholique de Louvain, October 1982.
18. U. K. Singh, 'A computation and comparison with measurements of transonic flow in an axial compressor stage with shock and boundary layer interaction'. *ASME Trans., A—J. Eng. Power*, **104,** (2), 510–515 (1982).
19. R. D. Richtmyer and K. W. Morton, *Difference methods for initial-value problems*, 2nd edn, Interscience Publishers, 1967.